A COMPARATIVE SEISMIC PERFORMANCE ASSESSMENT OF A MULTI-SPAN BRIDGE ISOLATED WITH ELASTOMERIC AND SLIDING ISOLATION SYSTEMS

COMPARACIÓN DEL DESEMPEÑO SÍSMICO DE UN PUENTE CONTINUO UTILIZANDO AISLADORES DEL TIPO ELASTOMÉRICO Y FRICCIONAL DESLIZANTE

Cristopher Trejo-Rodriguez[1]* , Carlos Melchor-Placencia[1]

¹Facultad de Ingeniería Civil, Universidad Nacional de Ingenieria, Lima, Peru

ABSTRACT

The remarkable performance of seismically isolated bridges in South America during the last two major seismic events has reflected the substantial increase in the adoption of base isolation in this type of infrastructure. In this paper, a non-isolated multi-span bridge was retrofitted for continued functionality adopting seismic isolation devices. With the aim of performing a comparative assessment of the most adopted base isolation techniques, the retrofitted bridge was analyzed using elastomeric and sliding isolation devices. In this case study, Lead Rubber Bearings (LRB) and Triple Friction Pendulum Bearings (TFPB) were selected as representative cases of elastomeric and sliding isolators, respectively. In the design of these isolation systems, the values of isolated periods, post-yield stiffness and yield force of both systems were set to be almost equals. This criterion was adopted for the purpose of comparing the unique effects of each type of isolator on the bridge seismic response. A series of nonlinear dynamic analyses were carried out considering both horizontal ground motion components to perform the comparative assessment. Numerical models that consider the bidirectional response and describe the different stages of motion of the isolators were adopted and then validated reproducing a series of benchmark tests. Upper and lower limit analyses were considered to gain a comprehensive understanding of the induced response by each isolation system. From the results, it is concluded that the LRB system induces a more uniform distribution of the seismic forces into the substructure; however, it experiences greater isolator displacements in comparison with the TFPB system.

Keywords: Seismic isolation, seismic response, nonlinear dynamic analysis, bridge

RESUMEN

El notable comportamiento de los puentes sísmicamente aislados en Sudamérica durante los dos últimos grandes eventos sísmicos, se ha visto reflejado en el aumento del uso de aisladores de base en este tipo de infraestructuras. En este trabajo, un puente no aislado de varios tramos fue reacondicionado para alcanzar una funcionalidad continua mediante la adopción de dispositivos de aislamiento sísmico. Con el objetivo de realizar una evaluación comparativa, se analizó el puente utilizando dispositivos de aislación del tipo elastomérico y deslizante. En este caso de estudio se escogió el aislador Elastomérico con Núcleo de Plomo (LRB) y el aislador Friccional de Triple Péndulo (TFPB) como modelos representativos. Para el diseño de ambos aisladores, se consideró que los valores de los periodos aislados, la rigidez post-fluencia y la fuerza de fluencia sean similares. Este criterio se adoptó con el fin de comparar los efectos únicos de cada tipo de aislador en la respuesta sísmica del puente. Se realizaron una serie de análisis dinámicos no lineales considerando las dos componentes del movimiento horizontal del suelo para realizar una evaluación comparativa. Se adoptaron modelos numéricos que consideran la respuesta bidireccional y describan las diferentes etapas de movimiento de los aisladores. Se consideraron análisis de límites superiores e inferiores para obtener una comprensión completa de la respuesta inducida por cada sistema de aislamiento. De los resultados, se concluye que el sistema LRB induce una distribución más uniforme de las fuerzas sísmicas en la subestructura; pero experimenta mayores desplazamientos en comparación con el sistema TFPB.

Palabras Clave: Aislación sísmica, respuesta sísmica, análisis dinámico no lineal, puentes

1. INTRODUCTION

Earthquakes are a significant threat to our society and as a response many innovative technologies have been developed for seismic hazard mitigation.

* Corresponding author:
lmoyah@uni.pe

Seismic isolation has proven to be a reliable design and retrofit strategy to improve the seismic performance. This design strategy has been widely adopted in South America since the 2010s. Several types of seismic isolators have been used in a range of bridge infrastructure projects with the aim of providing the lateral flexibility that lengthen the fundamental period of the structure to reduce the seismic demands drastically. In addition, these devices are capable of dissipating energy and providing lateral resistance to service loads.

Currently, the most widely used isolators in South American bridge infrastructure are the elastomeric and sliding bearings. Among these types of isolators, Lead-Rubber Bearing (LRB) and Friction Pendulum Bearing (FPB) are the most widely adopted. Despite having the same goal, the unique working mechanism is different in each case. LRBs lengthen the period of the structure by means of its rubber layers and dissipate energy by the melted state of its lead core. In contrast, FPBs dissipate energy through friction and shift the period due to the pendulum movement induced by its concave surfaces [1].

Previous works have been carried out to compare the different seismic performance levels induced by LRB and FPB isolation systems [2], [3]. However, these trends in the induced seismic responses have not been validated in the specific case of comparing Triple Friction Pendulum Bearings (TFPBs) with LRBs in isolated bridges.
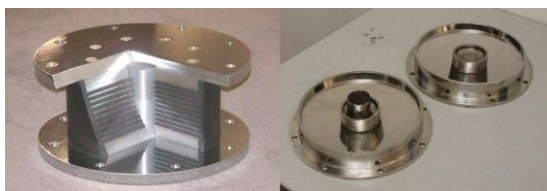

Fig. 1. Lead Rubber Bearing (LRB) and Triple Friction Pendulum Bearing (TFPB) [1].

With the aim of complementing the mainstream design practice of isolated bridges, two seismic isolation retrofitting solutions using LRBs and TFPBs were compared comprehensively. In this study, a comparative seismic performance assessment of an isolated three-span bridge was carried out using a deterministic approach. In the design of the isolators, a common design criteria, established by Eröz and DesRoches [2], were followed to compare the unique effects of each isolation system. In the numerical model of the isolated bridge, a simple bilinear hysteretic model was used to model the LRBs and an assemblage of

single friction pendulum bearings (SFPBs) for the TFPB modelling. A series of nonlinear time history analyses were performed considering seven ground motion records. From the results, the maximum isolator displacements (MID), the maximum isolator forces (MIF), the maximum distortions in the columns (MDC), the maximum accelerations in the deck (MAD), the maximum residual isolator displacements (MIR) and the maximum abutment-pier shear force ratio (MRF) were compared.

2. HYSTERETIC MODELING OF ISOLATORS

The hysteretic model developed by Bouc-Wen [4] is the basis to describe the hysteretic behavior of elastomeric and sliding isolators. In the case of LRBs, the hysteresis [5] is described through the following equation:

$$\begin{Bmatrix} F_{xe} \\ F_{ye} \end{Bmatrix} = K_d \begin{Bmatrix} u_x \\ u_y \end{Bmatrix} + c_d \begin{Bmatrix} \dot{u}_x \\ \dot{u}_y \end{Bmatrix} + \sigma_{YL(T)} A_L \begin{Bmatrix} Z_x \\ Z_y \end{Bmatrix} \qquad (1)$$

On other hand, the hysteretic behavior of SFPBs [6] is represented as follows:

$$\begin{Bmatrix} F_{xe} \\ F_{ye} \end{Bmatrix} = W \begin{Bmatrix} \dfrac{u_x}{R_x} \\ \dfrac{u_y}{R_y} \end{Bmatrix} + W \begin{Bmatrix} \mu_x Z_x \\ \mu_y Z_y \end{Bmatrix} \qquad (2)$$

Both hystereses depends on two dimensionless hysteretic variables, Z_x and Z_y, as proposed by Park et al. [7] for coupled bidirectional systems. These dimensionless variables are restricted to have a range and obeys a set of equations described by (3) and (4).

From equation (4), constants A, β and γ, called evolution constants, control the shape of the hysteretic loops.

To gain insight in the modelling of LRBs, the upper and lower bound approach adopted for the LRB case, that uses a simple bilinear hysteretic model [8], was compared with the results obtained with the model developed by Kalpakidis et al. [5]. This last model is able to capture the cycle-by-cycle strength reduction due to lead core heating effects. To perform this comparison, the hysteretic model which simulates the strength degradation [5] was implemented in MATLAB and the simple bilinear hysteresis was simulated using SAP2000 [8]. In this last hysteresis model, the upper and lower bound values of the LRB mechanical properties are considered through modification factors.

$$\sqrt{Z_x^2 + Z_y^2} \le 1 \qquad (3)$$

C. Trejo et al.

$$Y \begin{Bmatrix} \dot{Z}_x \\ \dot{Z}_y \end{Bmatrix} = \left(A[I] - \begin{bmatrix} Z_x^2(\gamma Sign(\dot{u}_x Z_x) + \beta) & Z_x Z_y(\gamma Sign(\dot{u}_y Z_y) + \beta) \\ Z_x Z_y(\gamma Sign(\dot{u}_x Z_x) + \beta & Z_y^2(\gamma Sign(\dot{u}_y Z_y) + \beta) \end{bmatrix} \right) \begin{Bmatrix} \dot{u}_x \\ \dot{u}_y \end{Bmatrix} \quad (4)$$

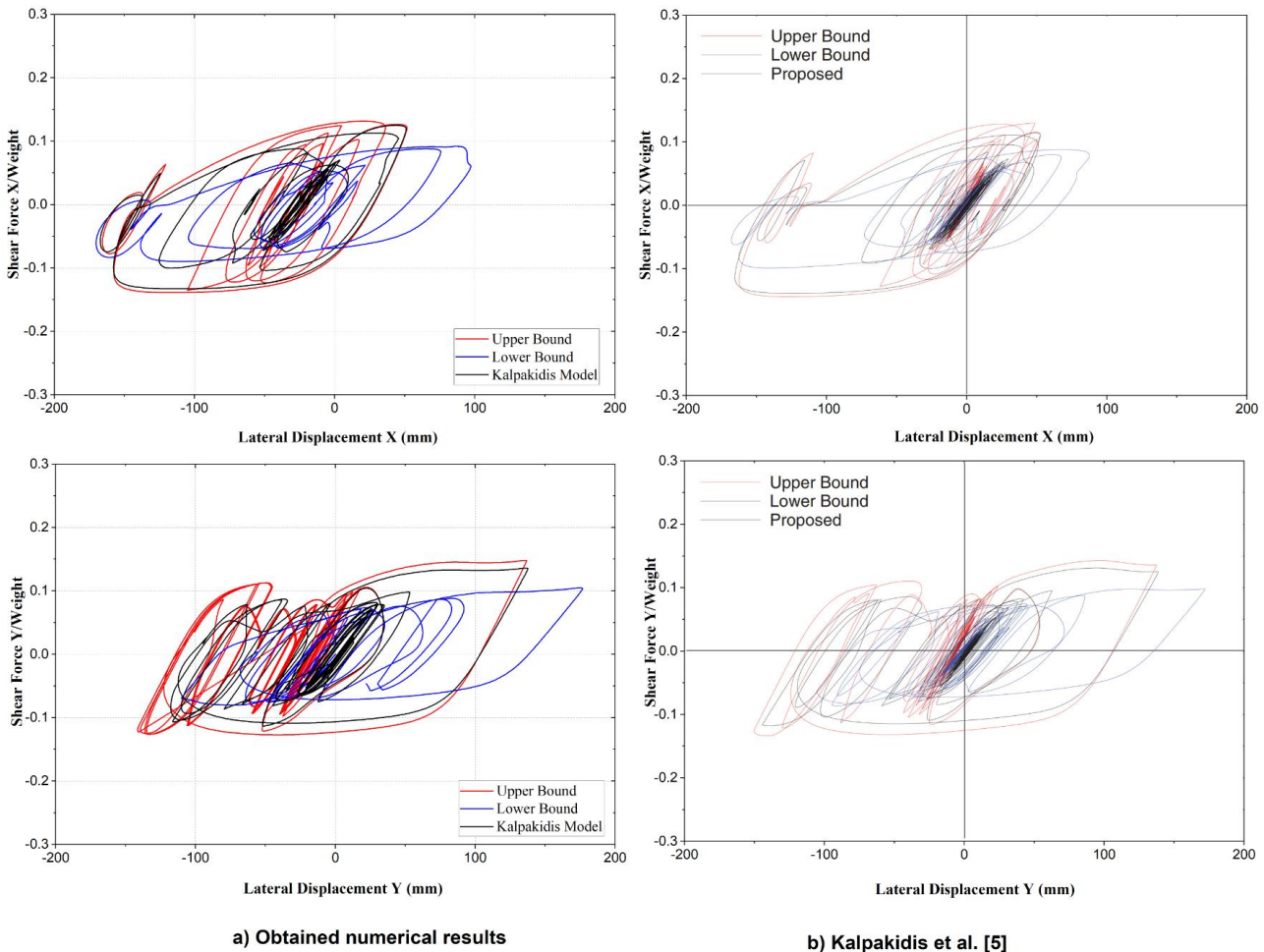a) Obtained numerical results   b) Kalpakidis et al. [5]

Fig. 2. LRB hysteresis loops obtained for the Duzce earthquake.

Previously, the implementation in MATLAB was validated [9] with the experimental and numerical results presented by Kalpakidis et al. [5]. The numerical results obtained for the Duzce earthquake seismic record (Turkey, 1978) are shown in Fig. 2. The derived results present a good agreement with the results obtained by Kalpakidis et al. [5], despite of using seismic records from different stations as it was not possible to obtain the same records of the authors. Therefore, the simple bilinear approach can be adopted to simulate the LRB behavior in the subsequent analyses with enough accuracy and less computational effort.

For friction pendulum isolators, the friction coefficient varies between a fast-sliding coefficient, μ_{max}, and a slow-sliding coefficient, μ_{min}. The relationship adopted to describe the variation of the friction coefficients, which depends also on a speed change parameter, r, are based on the experimental

results obtained by Nagarajaiah et al. [10] and described by the following equations:

$$\mu_x = \mu_{xmax} - (\mu_{xmax} - \mu_{xmin})e^{-r\dot{U}} \quad (5)$$

$$\mu_y = \mu_{ymax} - (\mu_{ymax} - \mu_{ymin})e^{-r\dot{U}} \quad (6)$$

To model the hysteretic behavior of TFPBs, an assembly of SFPBs should be performed. One approach uses SFPBs in parallel and the other in series. In this work, the series model implemented in SAP2000 was used.

In the process of gaining insight in the modeling of TFPBs, the validated numerical results from an experimental campaign performed by Becker [6] were adopted as benchmark results. Here, the results obtained for the Northridge seismic records are shown in Fig. 3 (USA, 1994). The obtained results have a good match with the verified numerical results.
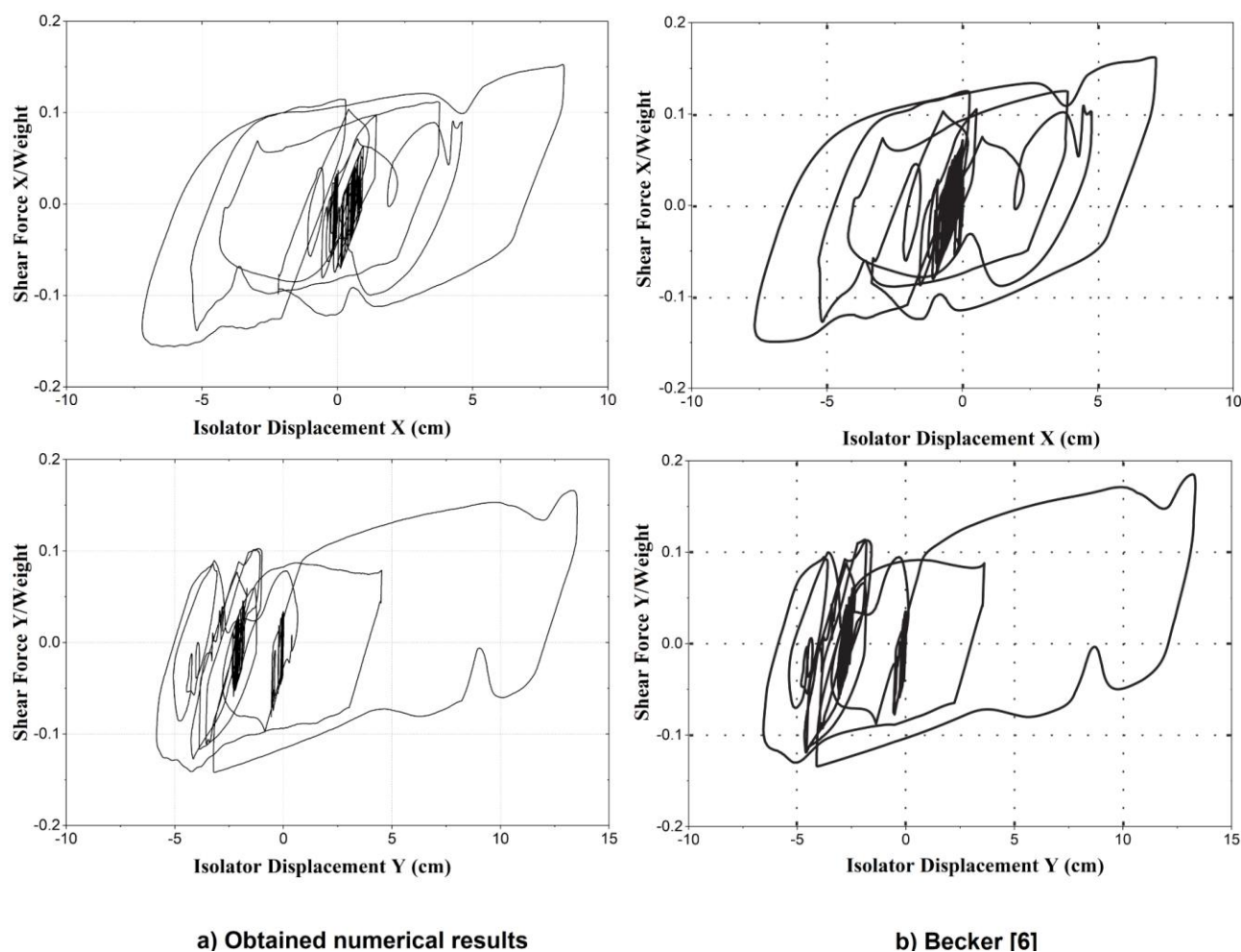
a) Obtained numerical results   b) Becker [6]

Fig. 3. TFPB hysteresis loops obtained for the Northridge earthquake.

3. DESIGN CRITERIA

A right three-span continuous composite highway bridge [11] was retrofitted adopting a seismic isolation solution to achieve continued functionality after a severe earthquake. Two retrofit strategies were studied, one using LRBs and the other using TFPBs. To perform a deep comparative assessment of the unique effects of each isolator, the design criteria set by Eröz and DesRoches [2] were followed. These criteria states that:

– The periods of both isolated bridges should be similar.
– The yield force and post-yield stiffness of each isolator should be almost similar.
– Uniform bearing sizes should be used in each isolation layout.

In this design, an isolated period of approximately 3 s was set. A displacement-based approach using a unimodal analysis method was adopted during the seismic isolation design [8]. In this case, it was considered that the supported deck of each isolated bridge is resting under two isolators in each support (piers and abutments). The resulting dimensions of the isolators are summarized in Table I and II.

TABLE I
Isolator properties LRB

	Pier	Abutment
Isolator diameter (m)	0.80	0.80
Lead core diameter (m)	0.14	0.14
Total thickness rubber (m)	0.30	0.30
Lead effective yield stress (MPa)	10	10
Shear modulus of rubber (MPa)	0.414	0.414

TABLE II
Isolator properties TFPB

	Pier	Abutment
Radius of curvature 1, 4 (m)	2.24	2.24
Radius of curvature 2, 3 (m)	0.41	0.41
Distance d1, d4 (m)	0.28	0.28
Distance d2, d3 (m)	0.05	0.05
Friction coefficient $\mu1, \mu4$	0.0685	0.0685
Friction coefficient $\mu2, \mu3$	0.0444	0.0444

4. NUMERICAL MODEL OF THE ISOLATED BRIDGE

The superstructure of the bridge is continuous and is made up of a steel-concrete composite deck as shown in Fig. 4. This deck consists of two side spans of 35 m and a central span of 50 m. The bridge substructure consists of two typical seat-type abutments and two intermediate piers made up of two circular columns (Fig. 5), which are 120 cm in diameter and 6.10 m in height, connected at the top with a 1.50 m deep cap beam. The total weight of the superstructure and substructure is 16760 kN and 1093 kN, respectively.
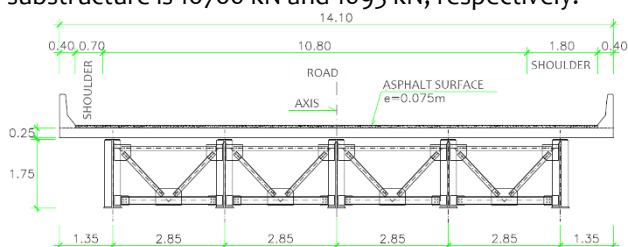
Fig. 4. Cross section of the superstructure.
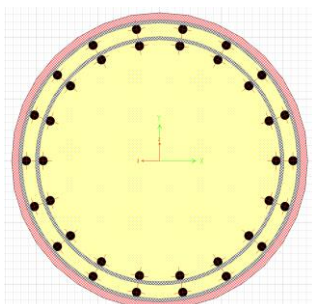
Fig. 5. Cross section of the column in the substructure.

In order to study the unique seismic response of the two seismic isolation retrofitting solutions for the bridge, two models of the structure were developed, called Model 1, for the LRB case, and Model 2, for the TFPB case.

Only beam-column and link elements were considered in the development of the numerical model (Fig. 6), labeled as stick model by Aviram et al. [12]. The superstructure (deck) was model with linear beam-column elements, as it remains in the linear elastic range. In the case of the substructure, the abutments were considered as rigids whereas the piers were assumed as flexible. The cap beams of the piers were modeled using linear beam-column elements whereas the columns were considered to enter into nonlinear range, so that beam-column elements with plastic hinges at its ends were adopted. A lumped plasticity model was considered for the hinges using the Clough's bilinear hysteretic model [13] shown in Fig. 7.
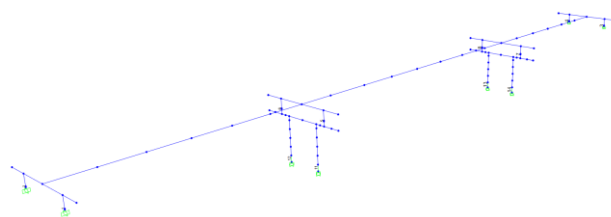

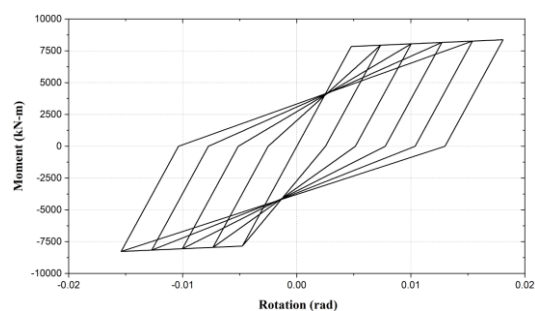Fig. 6. Three-dimensional modelling of the bridge.

Fig. 7. Clough's bilinear hysteretic model at column hinge.

The seismic isolators were modeled using link elements where the inelastic behavior is concentrated in a zero-length element which is connected to the bottom of the superstructure and the top of the substructure by means of rigid arms.

To obtain the moment-rotation curve of the plastic hinges in the columns, a moment-curvature analysis of the column cross section was performed. This curve depends on the geometric characteristics, the arrangement of the longitudinal and transverse reinforcing steel, the properties of the component materials and the axial load exerted on the section. The model of Mander et al. [14] was used to set the strain-stress curves for confined and unconfined concrete. For the longitudinal reinforcement, the model developed by Dodd and Restrepo [15] was adopted.

In order to estimate the right periods of the structure, the effective flexural stiffness of the columns was assessed using the results obtained from moment-curvature analysis. This effective stiffness is 57% of the gross section stiffness.

A set of nonlinear time-history analyses was performed according to the guidelines set by ASCE/SEI 7-16 [16]. These guidelines state that the Maximum Considered Earthquake (MCE) must be considered in the design. This earthquake has a 2% probability of being exceeded in a 50-year period, which means a recurrence period of approximately 2500 years. In this analysis, the design response spectrum established by the Peruvian Department of Transportation [17] was adopted as the target spectrum. This design spectrum represents a seismic hazard level of 7% probability of exceedance in 75 years. Seven pairs of near-fault seismic records (Table III) were selected for the dynamic analysis as they content large long-period pulses that induce considerable velocity and displacement demands into

the structure [18]. In order to attain the seismic-hazard level required, the design spectrum was scaled by a factor of 1.55 [9]. This factor was assessed using the mapped uniform hazard spectra provided in the SENCICO website [19]. After setting the target spectra, the seismic records were scaled to match it over a period range of interest (Fig. 8).
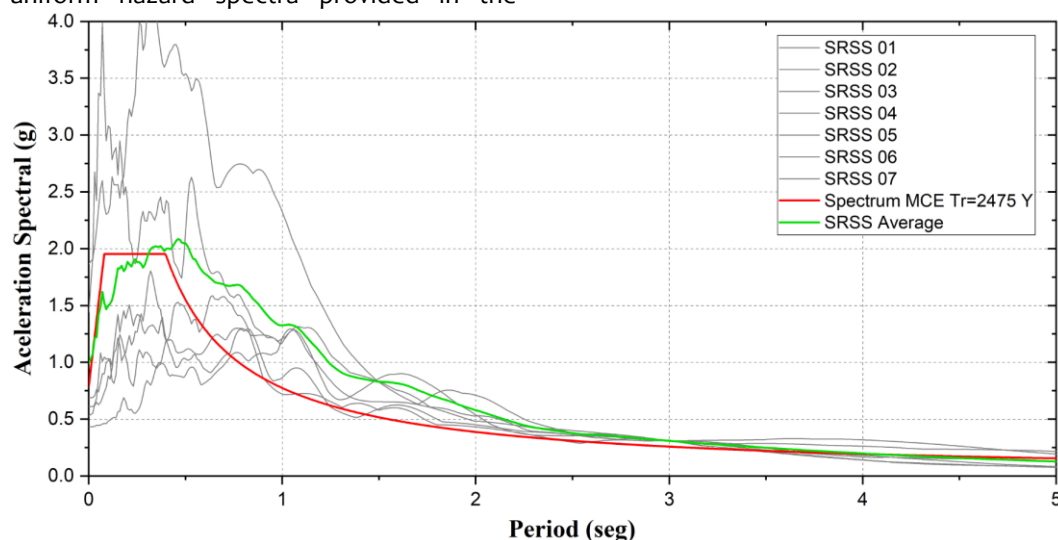

Fig. 8. SRSS elastic response spectrum of the 7 pairs seismic records and the MCE acceleration spectrum.

TABLE III
Seven pairs of ground motions used in the seismic analysis

Code PEER #	Name of the accelerogram	Station	M_W	R_{rup} (km)
RSN126	1976 Gazli USRR	Karakyr	6.8	5.46
RSN779	1989 Loma Prieta	LGPC	6.93	3.88
RSN803	1989 Loma Prieta	Saratoga, W. Valley Coll.	6.93	9.31
RSN982	1994 Northridge	Jensen Filter Plant	6.69	5.43
RSN1085	1994 Northridge	Sylmar, Coverter Sta. East	6.69	5.19
RSN1119	1995 Kobe Japan	Takarazuka	6.90	3.00
RSN1602	1999 Duzce Turkey	Bolu	7.14	12.4

The nonlinear analyses were performed using the Fast Nonlinear Analysis (FNA) method implemented and adopting a Rayleigh damping which overrides the isolated modes. This type of analysis is convenient due to the nature of the structure that concentrates the inelastic deformations only in the isolators, which allows obtaining computational accuracy and speed in comparison with other non-linear time-history methods [20].

5. NUMERICAL RESULTS

For the time-history analyses, the upper and lower bound properties were considered by means of modification factors. Through this way, the maximum absolute values in terms of displacement and shear forces were obtained. Table IV shows the lambda factors adopted in this analysis [21].

TABLE IV
Property modification factors for both isolators

	Lead Rubber		Friction Pendulum	
	G	σ_L	μ_{1-4}	μ_{2-3}
λ_{max}	1.83	1.84	2.12	2.12
λ_{min}	0.76	0.76	0.6	0.6

The isolators experienced the same seismic demands along the same transverse axis and symmetrically along the longitudinal axis. Therefore, the results are presented for one of the isolators located on one of the piers and one of the abutments. The isolator hysteresis from one of the nonlinear time history analyses is shown in Fig.9 and Fig.10.
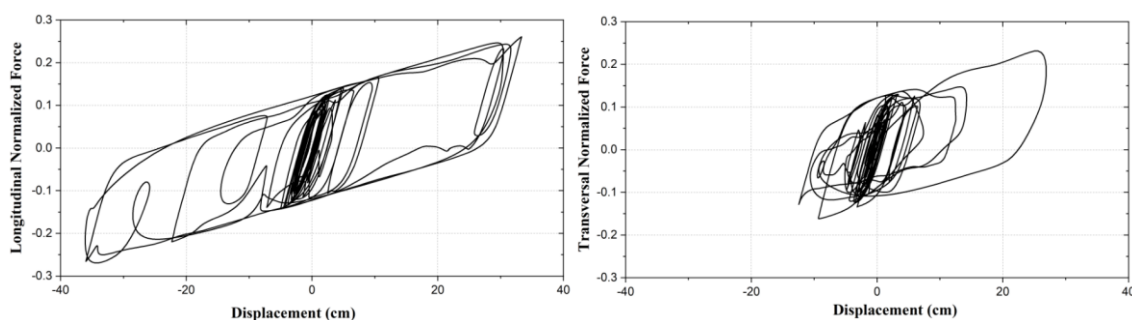

Fig. 9. Hysteresis loop for LRB at abutments (Bolu earthquake).
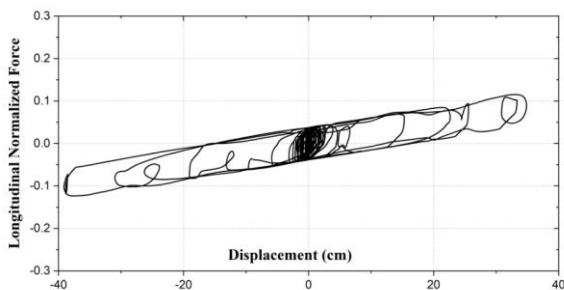
C. Trejo et al.

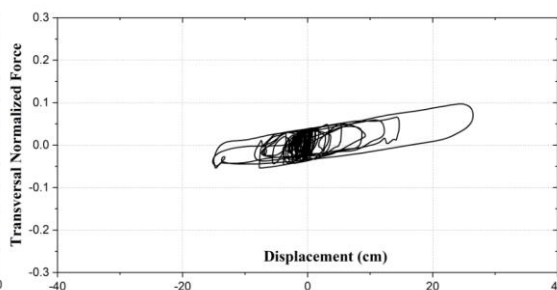Fig. 10. Hysteresis loop for TFPB at abutments (Bolu earthquake).

Fig. 11. Maximum isolator deformation (MID) on the top of the abutments.

The maximum absolute values of the seismic demands experienced in the isolators, deck and columns are: (1) the maximum isolator displacements (MID), (2) the maximum isolator forces (MIF), (3) the maximum distortions in the columns (MDC), (4) the maximum accelerations in the deck (MAD) or peak deck accelerations and (5) the maximum residual isolator displacements (MIR), which assess the self-centering capacity of the system. These maximum absolute values are shown in Fig. 11, Fig. 12, Fig. 13, Fig.14 and Fig.15. In addition, the maximum abutment-pier shear force ratio (MRF) was assessed to compare the shared shear force between the elements of the substructure (Fig.16). In these figures the mean values, and different cumulative percentiles of the seismic demands are plotted.

The MDC results show that the columns had not incursions into the inelastic range, as expected. In the LRB case, higher seismic demands were induced in the abutments, isolators, and bridge deck. In contrast, the TFPBs induced higher demands in the columns and self-centering capacity of the isolators. It should be pointed out that both isolator systems did not experienced damage as the LRBs did not exceed the deformation limit of 200% of their rubber height (82 cm) [22] and the TFPBs did not undergo beyond their fourth regimen of movement (81.5 cm) [23]. Also, it can be observed that the distribution of shear forces in the substructure was almost equal for the LRB case, which was not the case for the TFPBs.
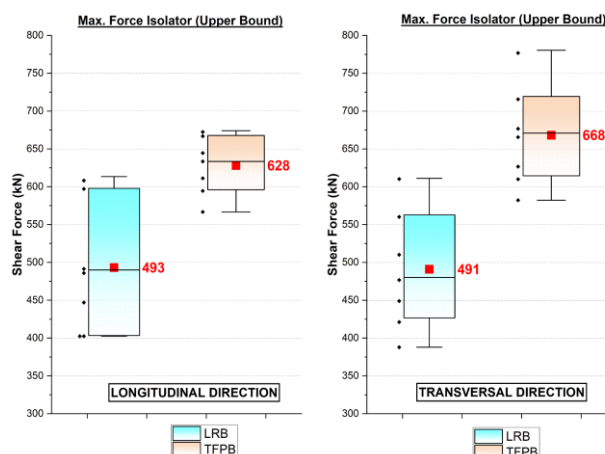

Fig. 12. Maximum isolator forces (MIF) on the top of the pier.
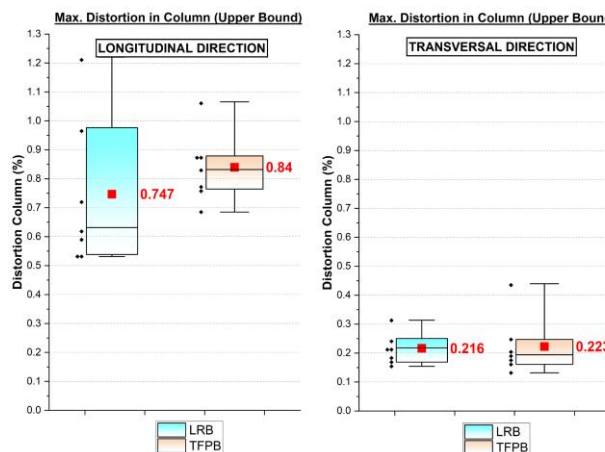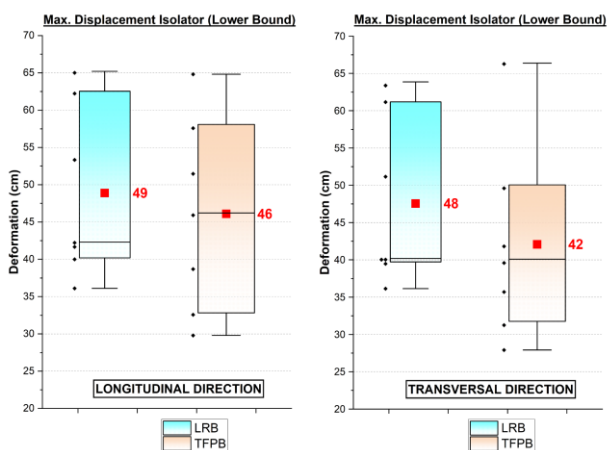
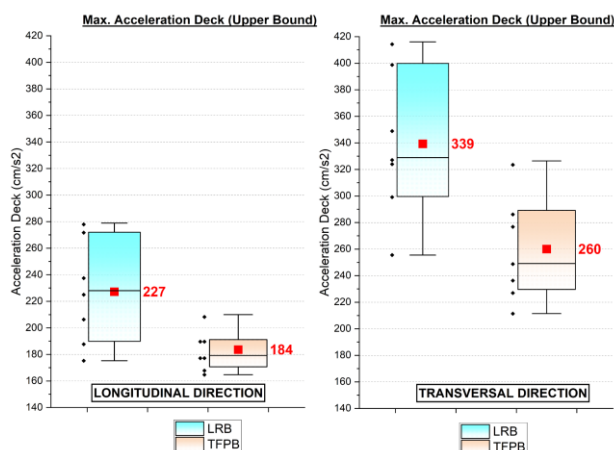

Fig. 13. Maximum distortions in the columns (MDC).

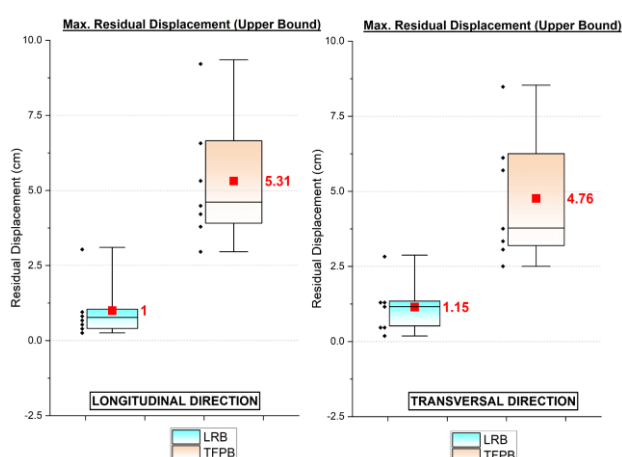Fig. 14. Maximum accelerations in the deck (MAD).

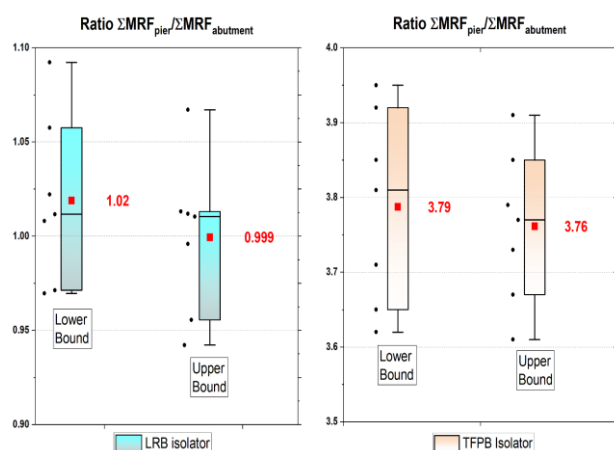
Fig. 15. Maximum residual isolator displacement (MIR).

Fig. 16. Maximum abutment-pier shear force ratio (MRF).

CONCLUSIONS

− From the analysis of the obtained results for both isolation systems, it is concluded that there are significant differences in the distribution of the different seismic demands in the superstructure and substructure components, despite of sharing common features both systems.

− The main difference in both isolation systems is the distribution of the shear forces along the substructure components. The results indicate that the LRBs induce a uniform distribution of the forces in comparison to the TFPB case. The non-uniform distribution in TFPBs is due to dependence of the frictional forces on the axial load supported in each isolator.

− From the results, it can be inferred that one isolation system performs better than the other depending on the engineering demand parameter (column drift, peak deck acceleration, self-centering capacity, induced shear forces) chosen in the seismic performance assessment.

− From previous comparative assessments in isolated bridges, it can be noticed that the overall trend in the induced seismic effects is mostly the same. However, further assessments are still required.

− The obtained results show that there is low variability in the maximum responses obtained with the seismic records used in this work. It can be concluded that the results obtained show a low dispersion and therefore their mean values represent reliable values.

REFERENCES

[1] M. Constantinou, I. Kalpakidis, A. Filiatrault, and R. A. Ecker Lay, "LRFD-Based Analysis and Design Procedures for Bridge Bearings and Seismic Isolators", MCEER Earthquake Engineering to Extreme Events, New York, USA, Sep. 2011.

[2] M. Eröz and R. DesRoches, "A Comparative Assessment of Sliding and Elastomeric Seismic Isolation in a Typical Multi-Span Bridge", Journal of Earthquake Engineering, vol 17, no. 5, pp. 637-657, Jul. 2013.

[3] F. Vilca, L. Quiroz and M. Torres, "Performance assessment of lead rubber bearing system and triple friction pendulum system at Piura's hospital, in Peru", 16th World Conference on Earthquake, 16WCEE 2017, Santiago, Chile, Jan. 2017.

[4] Y. K. Wen, "Method for random vibration of hysteretic systems", Journal of the Engineering Mechanics Division, Vol 102, no 2, pp. 249-263, Jun. 1976.

[5] I. Kalpakidis, M. Constantinou and A. Whittaker, "Modeling strength degradation in lead–rubber bearings under earthquake shaking", Earthquake Engineering and Structural Dynamics, Vol. 39, Buffalo, USA, Oct. 2010.

[6] T. C. Becker, "Advanced Modeling of the Performance of Structures Supported on Triple Friction Pendulum Bearings", University of California, Berkeley, USA, 2011.

[7] Y. J. Park, Y. K. Wen and A. Ang, "Random Vibration of Hysteretic Systems Under Bi-Directional Ground Motions", Earthquake Engineering and Structural Dynamics, Vol. 14, pp. 543-557, 1986.

[8] AASHTO, "Guide Specifications for Seismic Isolation Design. 4th Edition", Washington DC, USA, American

Association of Highway and Transportation Officials, 2014.

[9] C. Trejo, "Desempeño Sísmico de un Puente Continuo Típico con Aisladores del tipo Elastoméríco y Friccional Deslizante)", National University of Engineering, Lima, Perú, 2022.

[10] S. Nagarajaiah, A. M. Reinhorn and M. Constantinou, "Nonlinear Dynamics of Three-dimensional Base Isolated Structures (3D-BASIS)", National Center for Earthquake Engineering Research, New York, USA, Nov. 1989.

[11] C. Melchor, "Influencia de los Apoyos Elastoméricos en la Respuesta Sísmica de Puentes", National University of Engineering, Lima, Perú, 2016.

[12] A. Aviram, K. R. Mackie and B. Stojadinović, "Guidelines for Nonlinear Analysis of Bridge Structures in California", University of California, Berkeley, USA, Aug. 2008.

[13] S. A. Mahin and J. Lin, "Construction of Inelastic Response Spectra for Single-Degree-of-Freedom Systems", University of California, Berkeley, USA, Jun. 1983.

[14] J. Mander, M. Priestley and R. Park, "Theoretical Stress-Strain Model for Confined Concrete", Journal of Structural Engineering, Vol. 114, Sep. 1988.

[15] L. Dodd and J. Restrepo-Posada, "Model for Predicting Cyclic Behavior of Reinforcing Steel", Journal of Structural Engineering, Vol. 121, Mar. 1995.

[17] Ministerio de Transportes y Comunicaciones, "Manual de Puentes", Lima, Perú, Dec. 2018.

[18] M. Constantinou, A. S. Whittaker, D. M. Fenz and G. Apostolakis, "Seismic Isolation of Bridges", University at Buffalo, Buffalo, USA, Jun. 2007.

[19] SENCICO, "Generation of synthetic accelerograms for the coast of Peru. Specific Interinstitutional Cooperation Agreement Between the General Institute of Research of the National University of Engineering and the National Training Service for the Construction Industry –SENCICO", Lima, Perú, 2013.

[20] A. Sarlis and M. Constantinou, "Modeling Triple Friction Pendulum Isolators in Program Pap2000", University at Buffalo, Buffalo, USA, Jun. 2010.

[21] W. McVitty, and M. Constantinou, "Property Modification Factors for Seismic Isolators: Design Guidance for Buildings", MCEER Earthquake Engineering to Extreme Events, New York, USA, Jun. 2015.

[22] R. Tyler and W. Robinson, "High-Strain Tests on Lead-Rubber Bearings for Earthquake Loadings", Bulletin of the New Zealand Society for Earthquake Engineering, Vol. 17, pp. 90-105, Jun. 1984.

[23] D. M. Fenz and M. Constantinou, "Development, Implementation and Verification of Dynamic Analysis Models for Multi-Spherical Sliding Bearings", MCEER Earthquake Engineering to Extreme Events, New York, USA, Jun. 2008.